**BULLETIN** *of the*
MALAYSIAN MATHEMATICAL
SCIENCES SOCIETY
http://math.usm.my/bulletin

*Bull. Malays. Math. Sci. Soc. (2)* **35***(4) (2012), 945–959*

# Annulus with Circular Slit Map of Bounded Multiply Connected Regions via Integral Equation Method

[1]ALI W. K. SANGAWI, [2]ALI H. M. MURID AND [3]M. M. S. NASSER
[1,2]Ibnu Sina Institute for Fundamental Science Studies, Universiti Teknologi Malaysia,
81310 UTM Johor Bahru, Johor, Malaysia
[1,2]Department of Mathematics, Faculty of Science, Universiti Teknologi Malaysia,
81310 UTM Johor Bahru, Johor, Malaysia
[1]Department of Mathematics, College of Science, University of Sulaimani, 46001 UOS, Sulaimani, Kurdistan
[3]Department of Mathematics, Faculty of Science, Ibb University, P. O. Box 70270, Ibb, Yemen
[3]Department of Mathematics, Faculty of Science, King Khalid University, P. O. Box 9004, Abha, Saudi Arabia
[1]alisangawi2000@yahoo.com, [2]alihassan@utm.my, [3]mms_nasser@hotmail.com

**Abstract.** This paper presents a boundary integral equation method for the numerical conformal mapping of bounded multiply connected region onto an annulus with circular slits. The method is based on some uniquely solvable linear integral equations with classical, adjoint and generalized Neumann kernels. These boundary integral equations are constructed from a boundary relationship that relates the mapping function $f$ on a multiply connected region with $f'$, $\theta'$, and $|f|$, where $\theta$ is the boundary correspondence function. Some numerical examples are presented to illustrate the efficiency of the presented method.

2010 Mathematics Subject Classification: 30C30, 65E05

Keywords and phrases: Numerical conformal mapping, boundary integral equations, Neumann kernel, generalized Neumann kernel, multiply connected regions.

## 1. Introduction

Conformal mapping is a useful and important tool in science and engineering. On the other hand, exact mapping functions are unknown except for some special regions. By that fact, the practical use of conformal maps has always been limited. In general conformal maps cannot be obtained in closed form. Thus we have to resort to numerical approximations of such maps. Nowadays, much research has been done to discuss an algorithm for the constructions of conformal maps. Conformal mapping uses single valued functions of complex variables to transform a complicated boundary to a simpler, more manageable configuration. Nehari [19, p. 334] described five types of slit regions as important canonical regions for which a multiply connected region can be mapped onto. They are the annulus with circular slits, the disk with circular slits, the circular slit region, the radial slit region, and the parallel slit region. Various numerical approximation methods have been proposed for computing

*Communicated by* V. Ravichandran.
*Received:* September 12, 2011; *Revised:* December 29, 2011.

the conformal map between the multiply connected regions and the five canonical regions; see [1, 3, 5, 6, 8–10, 12–16, 20, 21, 24]. Murid and Mohamed [12] and Mohamed [11, pp. 51–88] have discussed a numerical conformal mapping of doubly connected regions onto an annulus via the Kerzman-Stein and Neumann kernels. Later, Murid and Hu [14] extend these works to multiply connected regions, which however, involves solving a nonlinear system of equation using optimization method. To overcome this nonlinear problem, Sangawi *et al.* [23] have developed linear integral equations for conformal mapping of bounded multiply connected regions onto a disk with circular slits. Recently, reformulations of conformal mappings from the bounded and unbounded multiply connected regions onto the five canonical slit regions as Riemann-Hilbert (RH) problems are discussed in Nasser [15–17]. An integral equation with the generalized Neumann kernel is then used to solve the RH problem as developed in [25]. The right-hand side of the integral equation however involves a singular integral which is computed by Wittich's method.

In this paper we describe an integral equation method for computing the conformal mapping function $f$ of multiply connected regions onto an annulus with circular slits. The approach presented improves significantly the results of [11–14]. We first derive a boundary relationship that relates the mapping function $f$ on a multiply connected region with $f'$, $\theta'(t)$, and $|f|$, where $\theta$ is the boundary correspondence function. We then construct three linear integral equations for $f'$, $\theta'(t)$, and $|f|$. This reduces the nonlinearity problem faced in [8, 14] to linear problem.

The plan of the paper is as follows: Section 2 presents some auxiliary materials and derivations of two integral equations related to $f'$. We derive in Section 3 a boundary integral equation satisfied by $\theta'$. Section 4 presents a method to calculate the modulus of $f$. Section 5 gives a numerical implementation for computing $f$ based on the computations of $\theta'$, modulus of $f$ and $f'(z)$. In Section 6, we give some examples to illustrate our boundary integral equation method. Finally, Section 7 presents a short conclusion.

## 2. Notations and auxiliary material

Let $\Omega$ be a bounded multiply connected region of connectivity $M+1$. The boundary $\Gamma$ consists of $M+1$ smooth Jordan curves $\Gamma_0, \Gamma_1, \ldots, \Gamma_M$ such that $\Gamma_1, \ldots, \Gamma_M$ lies in the interior of $\Gamma_0$ , where the outer curve $\Gamma_0$ has counterclockwise orientation and the inner curves $\Gamma_1, \ldots, \Gamma_M$ have clockwise orientation. The positive direction of the contour $\Gamma = \Gamma_0 \cup \Gamma_1 \cup \cdots \cup \Gamma_M$ is usually that for which $\Omega$ is on the left as one traces the boundary (see Figure 1). The curve $\Gamma_k$ is parametrized by $2\pi$-periodic twice continuously differentiable complex function $z_k(t)$ with non-vanishing first derivative, i.e.,

$$z_k'(t) = \frac{dz_k(t)}{dt} \neq 0, \quad t \in J_k = [0, 2\pi], \quad k = 0, 1, \ldots, M.$$

The total parameter domain $J$ is the disjoint union of $M+1$ intervals $J_0, \ldots, J_M$. We define a parametrization $z$ of the whole boundary $\Gamma$ on $J$ by

$$z(t) = \begin{cases} z_0(t), & t \in J_0 = [0, 2\pi], \\ \vdots & \\ z_M(t), & t \in J_M = [0, 2\pi]. \end{cases} \tag{2.1}$$

Let $H^*$ be the space of all real *Hölder* continuous $2\pi$-periodic functions $\omega(t)$ of the parameter $t$ on $J_k$ for $k = 0, 1, \ldots, M$, i.e.

$$\omega(t) = \begin{cases} \omega_0(t), & t \in J_0, \\ \vdots & \\ \omega_M(t), & t \in J_M. \end{cases}$$

Let $\theta(t)$ (the boundary corresponding function) be given for $t \in J$ by

$$\theta(t) = \begin{cases} \theta_0(t), & t \in J_0, \\ \vdots & \\ \theta_M(t), & t \in J_M. \end{cases}$$

Let $\mu$ (a picewise constant real function) be given for $t \in J$ by

$$\mu(t) = (\mu_0, \ldots, \mu_M) = \begin{cases} \mu_0, & t \in J_0, \\ \vdots & \\ \mu_M, & t \in J_M. \end{cases}$$

The classical Neumann kernel is defined by

$$N(t,s) = \frac{1}{\pi} \mathrm{Im}\left(\frac{z'(s)}{z(s) - z(t)}\right),$$

and the adjoint kernel $N^*(s,t)$ of the classical Neumann kernel is given by

$$N^*(t,s) = N(s,t) = \frac{1}{\pi} \mathrm{Im}\left(\frac{z'(t)}{z(t) - z(s)}\right).$$

We define the Fredholm integral operators $\mathbf{N}$ and $\mathbf{N}^*$ by

$$\begin{aligned} \mathbf{N}\upsilon(t) &= \int_J N(t,s)\upsilon(s)ds, \qquad t \in J, \\ \mathbf{N}^*\upsilon(t) &= \int_J N^*(t,s)\upsilon(s)ds, \qquad t \in J. \end{aligned}$$

It is known that $\lambda = 1$ is an eigenvalue of the kernel $N$ with multiplicity 1 and $\lambda = -1$ is an eigenvalue of the kernel $N$ with multiplicity $M$ [25]. The eigenfunctions of $N$ corresponding to the eigenvalue $\lambda = -1$ are $\left\{\chi^{[1]}, \chi^{[2]}, \ldots, \chi^{[M]}\right\}$, where

$$\chi^{[j]}(\xi) = \begin{cases} 1, & \xi \in \Gamma_j, \\ 0, & \text{otherwise}, \end{cases} \qquad j = 1, 2, \ldots, M.$$

Lastly, we define an integral operator $\mathbf{J}$ by

$$\mathbf{J}\upsilon = \int_J \frac{1}{2\pi} \sum_{j=1}^{M} \chi^{[j]}(s)\chi^{[j]}(t)\upsilon(s)ds, \tag{2.2}$$

which is required for uniqueness of solution in a later section.

The unit tangent to $\Gamma$ at $z(t)$ is denoted by $T(z(t)) = z'(t)/|z'(t)|$. Suppose that $c(z)$ and $Q(z)$ are complex-valued functions defined on $\Gamma$ such that $Q(z) \neq 0$. Then the interior relationship is defined as follows:

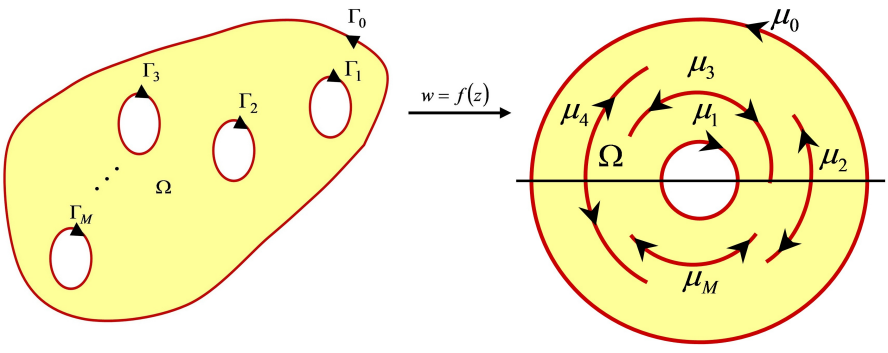


Figure 1. Mapping of the bounded multiply connected region $\Omega$ of connectivity $M$+1 onto an annulus with circular slits.

Let $P(z)$ be an analytic function in $\Omega$ and satisfies the boundary relationship

$$P(z) = c(z)\frac{\overline{T(z)Q(z)}}{\overline{G(z)}}\overline{P(z)}, \qquad z \in \Gamma, \tag{2.3}$$

where $G(z)$ analytic in $\Omega$, Hölder continuous on $\Gamma$, and $G(z) \neq 0$ on $\Gamma$. The boundary relationship (2.3) also has the following equivalent form:

$$G(z) = \overline{c(z)}T(z)Q(z)\frac{P(z)^2}{|P(z)|^2}, \qquad z \in \Gamma. \tag{2.4}$$

The following theorem from [8] gives an integral equation for an analytic function satisfying the boundary relationship (2.3) or (2.4).

**Theorem 2.1.** *Let $U$ and $V$ be any complex-valued functions that are defined on $\Gamma$. If the function $P(z)$ satisfies the interior non-homogeneous boundary relationship* (2.3) or (2.4), then

$$\frac{1}{2}\left[V(z) + \frac{U(z)}{\overline{T(z)Q(z)}}\right]P(z) + \mathrm{PV}\int_\Gamma K(z,w)P(w)|dw|$$

$$+c(z)U(z)\left[\sum_{a_j \text{inside}\Gamma}\operatorname*{Res}_{w=a_j}\frac{P(w)}{(w-z)G(w)}\right]^{\text{conj}} = 0, \qquad z \in \Gamma, \tag{2.5}$$

where

$$K(z,w) = \frac{1}{2\pi \mathrm{i}}\left[\frac{c(z)U(z)}{c(w)(\overline{w}-\overline{z})\overline{Q(w)}} - \frac{V(z)T(w)}{w-z}\right]. \tag{2.6}$$

The symbol "conj" in the superscript denotes complex conjugate. The sum in (2.5) is over all those zeros $a_1, a_2, \ldots, a_M$ of $G$ that lie inside $\Omega$. If $G$ has no zeros in $\Omega$, then the term containing the residue in (2.5) will not appear.

Let $w = f(z)$ be the analytic function which maps $\Omega$ conformally onto an annulus with circular slits. We assume that $a \in \Omega$. The function is made uniquely determined by prescribing that $f(a) > 0$ (see [19, p. 336]). The boundary value of $f$ can be represented in the

form

$$f(z_p(t)) = \mu_p e^{\mathrm{i}\theta_p(t)}, \quad \Gamma_p : z = z_p(t), \quad 0 \le t \le \beta_p, \quad p = 0,1,\ldots,M, \tag{2.7}$$

where $\theta_p$ is the boundary correspondence function of $\Gamma_p$. Thus it can be shown that [8]

$$f(z_p(t)) = \frac{\mu_p}{\mathrm{i}} T(z_p(t)) \frac{\theta_p'(t)}{|\theta_p'(t)|} \frac{f'(z_p(t))}{|f'(z_p(t))|}, \quad z_p \in \Gamma_p, \qquad p = 0,1,2,\ldots,M. \tag{2.8}$$

Note that $\theta_0' > 0$, $\theta_M' < 0$, but for $p = 1,2,\ldots,M-1$, $\theta_p'$ may be positive or negative since each circular slit $f(\Gamma_p)$ is traversed twice (see Figure 1). Thus $\theta_p'(t)/\left|\theta_p'(t)\right| = \operatorname{sign}(\theta_p'(t))$. Hence the boundary relationships (2.8) can be written as

$$f(z) = \operatorname{sign}(\theta_p'(t)) \frac{|f(z)|}{\mathrm{i}} T(z) \frac{f'(z)}{|f'(z)|}, \qquad z \in \Gamma. \tag{2.9}$$

Comparison of (2.4) and (2.9) leads to a choice of $G(z) = f(z)$, $P(z) = \sqrt{f'(z)}$, $c(z) = \mathrm{i}\operatorname{sign}(\theta_p'(t))\,|f(z)|$, $Q(z) = 1$. Note that since $f'(z) \neq 0$ in $\overline{\Omega}$, a single valued and analytic branch of $\sqrt{f'(z)}$ can be defined. Setting $U(z) = \overline{T(z)Q(z)}$ and $V(z) = 1$, Theorem 2.1 yields

$$\sqrt{f'(z)} + \mathrm{PV}\int_\Gamma K(z,w)\sqrt{f'(w)}\,|dw| = -c(z)\overline{T(z)} \times \left[\sum_{a_j \text{inside}\Gamma} \operatorname*{Res}_{w=a_j} \frac{\sqrt{f'(w)}}{(w-z)f(w)}\right]^{\mathrm{conj}}, \qquad z \in \Gamma, \tag{2.10}$$

where

$$K(z,w) = \frac{1}{2\pi\mathrm{i}}\left[\frac{c(z)\overline{T(z)}}{c(w)(\overline{w}-\overline{z})} - \frac{T(w)}{w-z}\right],$$

$$c(z) = \mathrm{i}\operatorname{sign}(\theta_p'(t))\,|f(z)|, \quad z = z(t),$$
$$c(w) = \mathrm{i}\operatorname{sign}(\theta_p'(s))\,|f(w)|, \quad w = z(s).$$

Note that $f(z)$ does not have any zeros in $\Omega$. Thus the right-hand side of (2.10) vanishes and the integral equation (2.10) becomes

$$\sqrt{f'(z)} + \mathrm{PV}\int_\Gamma K(z,w)\sqrt{f'(w)}\,|dw| = 0, \qquad z \in \Gamma. \tag{2.11}$$

Our approach here generalizes the results of Murid and Mohamed [12] and Hu [8]. In fact if $\Omega$ is doubly connected then the kernel $K(z,w)$ reduces to the following Kerzman-Stein-type kernel

$$A^*(z,w) = \frac{1}{2\pi\mathrm{i}}\left[\frac{|f(z)|\overline{T(z)}}{|f(w)|(\overline{w}-\overline{z})} - \frac{T(w)}{w-z}\right].$$

Relationship (2.9) is useful for computing the boundary values of the mapping function $f(z)$ provided $\theta_p'(t)$, $|f(z)|$, and $f'(z)$ are all known. Note that $|f(z_0)| = 1$, while $\left|f(z_q)\right| = \mu_q$, $q = 1,2,\ldots,M-1$ are the radii of the circular slits and $|f(z_M)| = \mu_M$ where $\mu_1,\ldots,\mu_M$ are undetermined real constants. Another integral equation method for calculating $f'(z)$ has

been given in Hu [8] and Murid and Hu [14]. They first eliminate the $\text{sign}(\theta_p'(t))$ in (2.9) by squaring both sides to get

$$f(z)^2 = -|f(z)|^2 T(z)^2 \frac{f'(z)^2}{|f'(z)|^2}, \qquad z \in \Gamma. \tag{2.12}$$

By means of Theorem 2.1 and (2.12), Murid and Hu [14] formulated the following boundary integral equation satisfied by $f'(z)$:

$$g_1(z,a) + \int_\Gamma N^+(z,w) g_1(w,a) |dw| = 0, \qquad z \in \Gamma, \tag{2.13}$$

where

$$\begin{aligned} g_1(z,a) &= T(z) f'(z), \\ N^+(z,w) &= \frac{1}{2\pi \mathrm{i}} \left[ \frac{T(z)}{z-w} - \frac{|f(z)|^2 \overline{T(z)}}{|f(w)|^2 (\overline{z}-\overline{w})} \right]. \end{aligned}$$

The integral equation (2.13) is similar to the integral equation for finding $f'$ in [23] but with different right-hand side. By using single-valuedness of the mapping function $f$ leads to the following condition

$$\int_{-\Gamma_q} g_1(w,a) |dw| = 0, \qquad q = 1,2,\ldots,M. \tag{2.14}$$

Note that the integral equation (2.13) with the condition (2.14) still are homogeneous. To overcome this problem we need to find another condition to change the above homogeneous integral equation to the non-homogeneous integral equation. To achieve this, we divide both sides of integral equation (2.13) and condition (2.14) by $f'(a)$, and we obtain

$$g(z,a) + \int_\Gamma N^+(z,w) g(w,a) |dw| = 0, \qquad z \in \Gamma, \tag{2.15a}$$

$$\int_{-\Gamma_q} g(w,a) |dw| = 0, \qquad q = 1,2,\ldots,M, \tag{2.15b}$$

where

$$g(z,a) = \frac{T(z) f'(z)}{f'(a)}.$$

By means of Cauchy's integral formula we can get the following condition

$$\int_\Gamma \frac{1}{2\pi} \frac{g(w,a)}{w-a} |dw| = \mathrm{i}. \tag{2.15c}$$

Thus the integral equation (2.15a) with the conditions (2.15b) and (2.15c) should give a unique solution provided the parameters $\left|f(z_q)\right| = \mu_q$, $q = 1,2,\ldots,M$ that appear in $N^+(z,w)$ are known.

Integral equation methods for computing $\theta_p'$ and $\left|f(z_q)\right| = \mu_q$ are discussed in the next two sections.

## 3. Integral equation method for computing $\theta_p^{'}(t)$

This section gives another application of Theorem 2.1 for computing $f'/f$. Let $f(z)$ be the mapping function as described before. The function $f$ can also be written as

$$f(z) = (z - z_0)e^{g(z)}, \tag{3.1}$$

where $a \in \Omega$, $z_0 \in$ interior of $\Gamma_M$, $g$ is an analytic in $\Omega$ and $\alpha$ is real constant. It is clear from (2.7) that $f'(z_p(t))z_p'(t)/f(z_p(t)) = \mathrm{i}\theta_p^{'}(t)$. An integral equation method for calculating $f'(z)/f(z)$, $z \in \Gamma$, is given next. Then the function $D(z)$ defined by

$$D(z) = \frac{f'(z)}{f(z)} = g'(z) + \frac{1}{z - z_0}, \tag{3.2}$$

is analytic in $\Omega$.

Combining (2.12) and (3.2), we obtain the following boundary relationship

$$D(z) = -\overline{T(z)}^2\,\overline{D(z)}, \qquad z \in \Gamma. \tag{3.3}$$

Comparison of (2.3) and (3.3) leads to a choice of $P(z) = D(z)$, $Q(z) = T(z)$, $c(z) = -1, G(z) = 1$. Setting $U(z) = \overline{T(z)Q(z)}$ and $V(z) = 1$, Theorem 2.1 yields

$$\frac{f'(z)}{f(z)}T(z) + \mathrm{PV}\frac{1}{2\pi\mathrm{i}}\int_\Gamma \left[\frac{T(z)}{z-w} - \frac{\overline{T}(z)}{\overline{z}-\overline{w}}\right]\frac{f'(w)}{f(w)}T(w)\,|dw| = 0, \quad z \in \Gamma. \tag{3.4}$$

In the above integral equation let $z = z(t)$ and $w = z(s)$. Then by multiplying both sides of (3.4) by $|z'(t)|$ and using the fact that

$$\frac{f'(z(t))}{f(z(t))}z'(t) = \mathrm{i}\theta'(t),$$

the above integral equation can also be written as

$$\theta'(t) + \int_J N(s,t)\theta'(s)ds = 0.$$

This integral equation is similar to the integral equation for finding $\theta'(t)$ in [23] but with different right-hand side. Since $N(s,t) = N^*(t,s)$, the integral equation can be written as an integral equation in operator form

$$(\mathbf{I} + \mathbf{N}^*)\theta' = 0, \tag{3.5}$$

where $\lambda = -1$ is an eigenvalue of $N^*$ with multiplicity $M$ by Theorem 12 in [25]. By using the fundamental theorem [22, p.164] and using the fact that $T(w)\,|dw| = dw$, gives

$$\int_{-\Gamma_p} \frac{1}{2\pi}T(w)\frac{f'(w)}{f(w)}\,|dw| = \begin{cases} \mathrm{i}, & p = M, \\ 0, & p = 1,2,\ldots,M-1, \end{cases} \tag{3.6}$$

which implies that

$$\mathbf{J}\theta' = (0,\ldots,0,-1). \tag{3.7}$$

By adding (3.7) to (3.6), we obtain the equation

$$(\mathbf{I} + \mathbf{N}^* + \mathbf{J})\theta' = \hat{\phi}(t), \tag{3.8}$$

where

$$\hat{\phi}(t) = (0,\ldots,0,-1). \tag{3.9}$$

The integral equation (3.8) is uniquely solvable (see [23]).

## 4. Integral equation for computing $|f(z)|$

The boundary values of $f$ satisfy on the boundary $\Gamma$,

$$f(z(t)) = \mu(t)e^{i\theta(t)}, \tag{4.1}$$

where $\mu(t) = (1, \mu_1, \ldots, \mu_M)$.

By taking the logarithm on both sides of (3.1), we get

$$\log f(z) = \log(z - z_0) + g(z). \tag{4.2}$$

Then

$$\begin{aligned} g(z(t)) &= \ln\mu(t) - \ln|z(t) - z_0| - i\arg(z(t) - z_0) + i\theta(t) \\ &= \gamma(t) + h(t) + i\upsilon, \end{aligned} \tag{4.3}$$

where $\gamma(t) = -\ln|z(t) - z_0|$ and $h(t) = \ln\mu(t) = (0, \ln\mu_1, \ln\mu_2, \ldots, \ln\mu_M)$. This choice of $\gamma(t)$ is different from the one chosen in [23] which is related to disk with circular slits.

The following theorem gives a method for calculating $h(t)$ and hence $\mu(t)$. This theorem can be proved by using the approach used in proving Theorem 5 in [18].

**Theorem 4.1.** *The function $h$ is given by $h = (0, h_1, h_2, \ldots, h_M)$, where*

$$h_j = (\gamma, \phi^{[j]}) = \frac{1}{2\pi}\int_J \gamma(t)\phi^{[j]}(t)dt\ , \tag{4.4}$$

*and where $\phi^{[j]}$ is the unique solution of the following integral equation*

$$(\mathbf{I} + \mathbf{N}^* + \mathbf{J})\phi^{[j]} = -\chi^{[j]}\ , \qquad j = 1, 2, \ldots, M. \tag{4.5}$$

*By obtaining $h_1, h_2, \ldots, h_M$, we obtain*

$$\mu_j = e^{h_j}\ , \qquad j = 1, 2, \ldots, M. \tag{4.6}$$

In summary, by solving the integral equation (3.4) with the condition (3.6) we get $\theta_p'(t)$. And solving the integral equation (4.5) we get $\phi^{[r]}$, $r = 1, 2, \ldots, M$, which gives $h_r$ through (4.4) which in turn gives $\mu_r$ through (4.6). By solving integral equation (2.15a) with the conditions (2.15b) and (2.15c) with the known values of $\mu_r$ we get $g(z, a)$. From the definition of $g(z, a)$, we get

$$f'(z) = \frac{g(z, a)f'(a)}{T(z)}. \tag{4.7}$$

Note that, from the solution of (3.4) and (3.6) it is possible to compute

$$\frac{f'(a)}{f(a)} = \frac{1}{2\pi i}\int_\Gamma \frac{f'(w)}{f(w)(w - a)}dw. \tag{4.8}$$

Finally from (2.8), (4.7) and (4.8), the boundary value of $f(z)$ is given by

$$f(z) = \operatorname{sign}(\theta'(t))\frac{|f(z)|}{i}\frac{g(z, a)f'(a)/f(a)}{|g(z, a)f'(a)/f(a)|}, \qquad z \in \Gamma. \tag{4.9}$$

The interior value of the function $f(z)$ is calculated by the Cauchy integral formula

$$f(z) = \frac{1}{2\pi i}\int_\Gamma \frac{f(w)}{w - z}dw, \qquad z \in \Omega. \tag{4.10}$$

For points $z$ which are not close to the boundary, the integral in (4.10) is approximated by the trapezoidal rule. However for the points $z$ closed to the boundary $\Gamma$, the numerical integration in (4.10) is nearly singular. This difficulty is overcome by using the fact that $(2\pi\mathrm{i})^{-1}\int_\Gamma dw/(w-z)=1$, and rewrite $f(z)$ as

$$f(z)=\frac{\int_\Gamma \frac{f(w)}{w-z}dw}{\int_\Gamma \frac{1}{w-z}dw}, \qquad z\in\Omega. \tag{4.11}$$

This idea has the advantage that the denomenator in this formula compensates for the error in the numerator (see [7]). The integrals in (4.11) are approximated by the trapezoidal rule.

## 5. Numerical examples

Since the function $z_p(t)$ is $2\pi$-periodic, a reliable procedure for solving the integral equations (2.15), (3.8) and (4.5) numerically is by using the Nyström's method with the trapezoidal rule [2]. The trapezoidal rule is the most accurate method for integrating periodic functions numerically [4, pp. 134–142]. Thus solving the integral equations numerically reduces to solving linear systems of the form

$$AX=B. \tag{5.1}$$

The above linear system (5.1) is uniquely solvable for sufficiently large number of collocation points on each boundary component, since the integral equations (2.15), (3.8) and (4.5) are uniquely solvable [2]. The computational details are similar to [15, 23].

For numerical experiments, we have used some test regions of connectivity two, three, four and five based on the examples given in [1, 5, 9, 15, 16, 21, 22]. All the computations were done using MATHEMATICA 7.1 (16 digit machine precision). The number of points used in the discretization of each boundary component $\Gamma_j$ is $n$. The test regions and their corresponding images are shown in Figures 2-6.

### 5.1. Regions of connectivity two

In this section we have used one test region of connectivity two whose exact mapping function is known. The test region is the circular frame. The results for sub norm error between the exact values of $f$, $\mu_1$ and approximate values $f_n$, $\mu_{1n}$ are shown in Table 1.

**Example 5.1.** Circular Frame :
Consider a pair of circles

$$\begin{aligned}\Gamma_0 : \{z(t) &= e^{\mathrm{i}t}\},\\ \Gamma_1 : \{z(t) &= c+\rho e^{-\mathrm{i}t}\}, \qquad t: 0\le t\le 2\pi, \quad z_0=0.3,\end{aligned}$$

such that the domain bounded by $\Gamma_0$ and $\Gamma_1$ is the domain between a unit circle and a circle centered at $c$ with radius $\rho$ [22]. The exact mapping function is given by

$$f(z)=\frac{z-\lambda}{\lambda z-1}, \tag{5.2}$$

with

$$\lambda=\frac{2c}{1+(c^2-\rho^2)+\sqrt{(1-(c-\rho)^2)(1-(c+\rho)^2)}},$$

which maps $\Gamma_0$ onto the unit circle and $\Gamma_1$ onto a circle of radius

$$\mu_1 = \frac{2\rho}{1-(c^2-\rho^2)+\sqrt{(1-(c-\rho)^2)(1-(c+\rho)^2)}}.$$

Figure 2 shows the region and its image based on our method. See Table 1 for results.

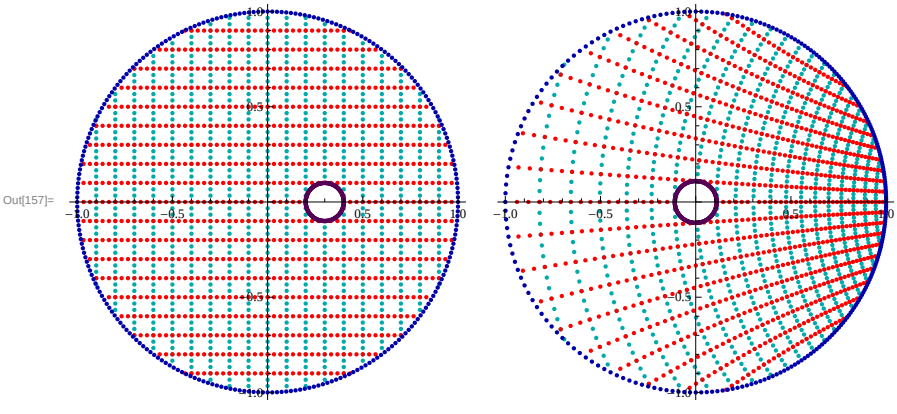


Figure 2. Conformal mapping of a circular frame onto an annulus.

Table 1. Error Norm (Circular Frame).

| $n$ | $\|\mu_1-\mu_{1n}\|_\infty$ | $\|f-f_n(t)\|_\infty$ |
|---|---|---|
| 4 | 2.2(−03) | 6.5(−02) |
| 8 | 2.2(−05) | 1.4(−03) |
| 16 | 1.9(−09) | 2.2(−07) |
| 32 | 8.3(−17) | 1.2(−15) |

### 5.2. Regions connectivity three

In this section we have used two test regions of connectivity three whose exact mapping functions are unknown. The first test region is bounded by an ellipse and two circles and the second test region is bounded by two ellipses and a circle. The results for sub norm error between the our numerical values of $\mu_1$, $\mu_2$ and the computed values of $\mu_1$, $\mu_2$ obtained from [5, 9, 15, 16, 21] are shown in Tables 2 and 3.

**Example 5.2.** Ellipse with Two Circles:
Let $\Omega$ be the region bounded by

$$\begin{aligned}
\Gamma_0 : \{z(t) &= 2\cos t + \mathrm{i}\sin t\},\\
\Gamma_1 : \{z(t) &= 0.5\,(\cos t - \mathrm{i}\sin t)\,\},\\
\Gamma_2 : \{z(t) &= 1.2 + 0.3\,(\cos t - \mathrm{i}\sin t)\,\}, \qquad 0 \le t \le 2\pi.
\end{aligned}$$

This example is also discussed in Nasser [16] which allows for comparison of the radii $\mu_1$, $\mu_2$, where $\mu_1 = 2.3741142722$, $\mu_2 = 1.2497448086$. Since our condition of the problem is different from him so we should multiply our radii by 2.5 to compare with the result of Nasser [16]. We choose the symbols $\mu_{1R}$ and $\mu_{2R}$ for the radii in Nasser [16]. Figure 3 shows the region and its image based on our method. See Tables 2 for comparison of our computed values of $\mu_1$ and $\mu_2$ with those computed values of Nasser [16].

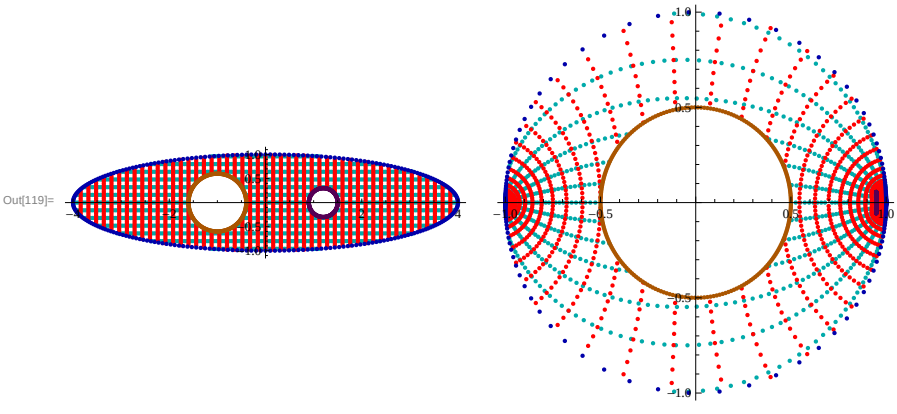


Figure 3. Mapping a region $\Omega$ bounded by an ellipse and two circles onto an annulus with a circular slit.

Table 2. Radii comparison for Example 5.2 with [16].

| $n$ | $\|\mu_1 \times 2.5 - \mu_{1R}\|_\infty$ | $\|\mu_2 \times 2.5 - \mu_{2R}\|_\infty$ |
|---|---|---|
| 32 | 5.0(−05) | 8.9(−04) |
| 64 | 3.8(−07) | 8.7(−07) |
| 128 | 8.6(−13) | 1.8(−11) |

**Example 5.3.** Two Ellipses with One Circle:
Let $\Omega$ be the region bounded by

$$\begin{aligned}
\Gamma_0 : \{z(t) &= 2\cos t + \mathrm{i}\sin t\},\\
\Gamma_1 : \{z(t) &= -0.7{+}0.25\,(\cos t - \mathrm{i}\sin t)\,\},\\
\Gamma_2 : \{z(t) &= 1 + 0.5\cos t - 0.25\mathrm{i}\sin t\}, \qquad 0 \le t \le 2\pi, \quad z_0 = 1.
\end{aligned}$$

Figure 4 shows the region and its image based on our method. See Table 3 for comparison between our computed values of $\mu_1$ and $\mu_2$ with those computed values of Nasser [15].

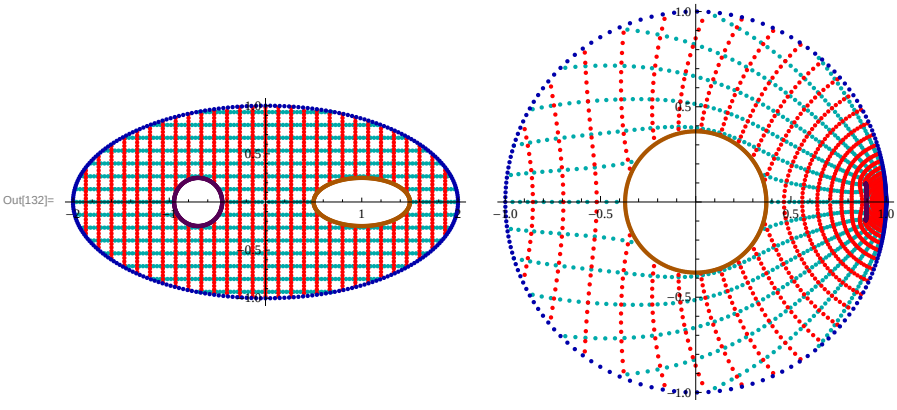


Figure 4. Mapping a region Ω bounded by two ellipses and one circle onto an annulus with a circular slit.

Table 3. Error Norm for Example 5.3.

| $n$ | $\|\mu_1-\mu_{1N}\|$ | $\|\mu_2-\mu_{2N}\|$ |
|---|---|---|
| 16 | 1.0(−04) | 6.1(−05) |
| 48 | 1.4(−12) | 3.4(−13) |
| 64 | 1.4(−15) | 1.1(−15) |

### 5.3. Regions of connectivity four and five

In this section we have used two test regions for multiply connected regions whose exact mapping functions are unknown. The first test region is as shown in Figure 5 and the second test region is bounded by an ellipse and four circles [15]. The computed values of $\mu_1$, $\mu_2$, $\mu_3$, $\mu_4$ are shown in Tables 4 and 5.

**Example 5.4.** Let Ω be the region bounded by

$$\begin{aligned}
\Gamma_0 : \{z(t) &= (10+3\cos 3t)e^{\mathrm{i}t}\},\\
\Gamma_1 : \{z(t) &= -3.5+6\mathrm{i}+0.5e^{\frac{-i\pi}{4}}(e^{\mathrm{i}t}+4e^{-\mathrm{i}t})\},\\
\Gamma_2 : \{z(t) &= 5+0.5e^{\frac{\mathrm{i}\pi}{4}}(e^{\mathrm{i}t}+4e^{-\mathrm{i}t})\},\\
\Gamma_3 : \{z(t) &= -3.5-6\mathrm{i}+0.5e^{\frac{\mathrm{i}\pi}{4}}(e^{\mathrm{i}t}+4e^{-\mathrm{i}t})\}, \qquad 0\le t\le 2\pi,\ z_0=-4-6\mathrm{i}.
\end{aligned}$$

This example is also discussed in Nasser [15]. See Figure 5 shows the region and its image based on our method. See Table 4 for results.

**Example 5.5.** Ellipse with Four Circles:
Let Ω be the region bounded by

$$\begin{aligned}
\Gamma_0 : \{z(t) &= 8\cos t+6\mathrm{i}\sin t\},\\
\Gamma_1 : \{z(t) &= 3+2\mathrm{i}+\cos t-\mathrm{i}\sin t\},
\end{aligned}$$

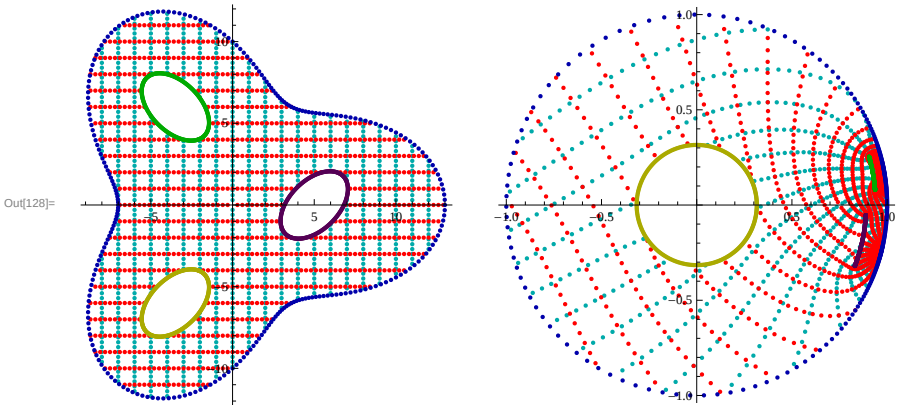


Figure 5. Mapping a region $\Omega$ onto an annulus with two circular slits.

Table 4. The numerical values of $\mu_1$, $\mu_2$ and $\mu_3$.

| $n$ | $\mu_1$ | $\mu_2$ | $\mu_3$ |
|---|---|---|---|
| 32 | 0.9400798851906385 | 0.8899301609674942 | 0.3155456958536308 |
| 64 | 0.9400786116038745 | 0.8899315928064306 | 0.3155455847860195 |
| 128 | 0.940078611605828 | 0.8899315927710835 | 0.3155455847853972 |

$$\begin{aligned}\Gamma_2 : \{z(t) &= -3+2\mathrm{i}+\cos t-\mathrm{i}\sin t\},\\ \Gamma_3 : \{z(t) &= -3-2\mathrm{i}+\cos t-\mathrm{i}\sin t\},\\ \Gamma_4 : \{z(t) &= 3-2\mathrm{i}+\cos t-\mathrm{i}\sin t\}, \qquad 0\le t\le 2\pi,\ z_0=-3-2\mathrm{i}.\end{aligned}$$

This example is also discussed in Nasser [15]. Figure 6 shows the region and its image based on our method. See Table 5 for results.

Table 5. The numerical values of $\mu_1$, $\mu_2$, $\mu_3$ and $\mu_4$.

| $n$ | $\mu_1$ | $\mu_2$ | $\mu_3$ | $\mu_4$ |
|---|---|---|---|---|
| 32 | 0.84922711665091 | 0.63729798437032 | 0.210432179308122 | 0.80742128277745 |
| 64 | 0.84922717271639 | 0.6372980012645 | 0.210432177445509 | 0.80742132924948 |
| 128 | 0.84922717271638 | 0.63729800126452 | 0.210432177445504 | 0.80742132924948 |

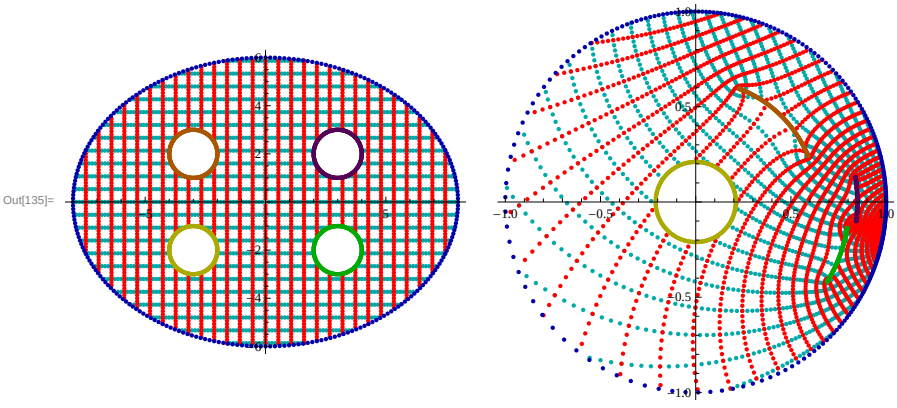


Figure 6. Mapping a region Ω bounded by an ellipse and four circles onto an annulus with three circular slits.

## 6. Conclusion

In this paper, we have constructed new boundary integral equation method for conformal mapping of multiply connected regions onto an annulus with circular slits. We have also constructed a new method to find the values of circular radii that reduces the nonlinearity problem encountered in Murid and Hu [8] to linear problem. By solving the integral equations, we obtains the values of $\theta'$, $|f|$ and $f'$ which in turn gives the approximate boundary value of the mapping function. These integral equations are similar to the integral equations in [23] for disk with circular slits but with different right-hand sides. Furthermore the right-hand sides of the integral equations do not involve any singularity. The interior mapping function are calculated by the means of the Cauchy integral formula. Several mappings of the test regions of connectivity two, three, four and five were computed numerically using the proposed method. The numerical examples presented have illustrated that our boundary integral equation method has high accuracy.

**Acknowledgement.** This work was supported in part by the Malaysian Ministry of Higher Education (MOHE) through the Research Management Centre (RMC), Universiti Teknologi Malaysia (FRGS Votes 78346, 78479). This support is gratefully acknowledged. We wish to thank an anonymous referee for valuable comments and suggestions on the manuscript which improve the presentation of the paper.

## References

[1] K. Amano, A charge simulation method for the numerical conformal mapping of interior, exterior and doubly-connected domains, *J. Comput. Appl. Math.* **53** (1994), no. 3, 353–370.

[2] K. E. Atkinson, *The Numerical Solution of Integral Equations of the Second Kind*, Cambridge Monographs on Applied and Computational Mathematics, 4, Cambridge Univ. Press, Cambridge, 1997.

[3] D. Crowdy and J. Marshall, Conformal mappings between canonical multiply connected domains, *Comput. Methods Funct. Theory* **6** (2006), no. 1, 59–76.

[4] P. J. Davis and P. Rabinowitz, *Methods of Numerical Integration*, second edition, Computer Science and Applied Mathematics, Academic Press, Orlando, FL, 1984.

[5] S. W. Ellacott, On the approximate conformal mapping of multiply connected domains, *Numer. Math.* **33** (1979), no. 4, 437–446.
[6] P. Henrici, *Applied and Computational Complex Analysis*, Wiley-Interscience, New York, 1974.
[7] J. Helsing and R. Ojala, On the evaluation of layer potentials close to their sources, *J. Comput. Phys.* **227** (2008), no. 5, 2899–2921.
[8] L. Hu, Boundary Integral Equations Approach for Numerical Conformal Mapping of Multiply Connected Regions, PhD Thesis, Department of Mathematics, Universiti Teknologi Malaysia, 2009.
[9] C. A. Kokkinos, N. Papamichael and A. B. Sideridis, An orthonormalization method for the approximate conformal mapping of multiply-connected domains, *IMA J. Numer. Anal.* **10** (1990), no. 3, 343–359.
[10] P. K. Kythe, *Computational Conformal Mapping*, Birkhäuser Boston, Boston, MA, 1998.
[11] N. A. Mohamed, An Integral Equation Method for Conformal Mapping of Doubly Connected Regions via the Kerzman-Stein and the Neumann Kernels, Master Thesis, Department of Mathematics, Universiti Teknologi Malaysia, 2007.
[12] A. H. M. Murid and N. A. Mohamed, Numerical conformal mapping of doubly connected regions via the Kerzman-Stein kernel, *Int. J. Pure Appl. Math.* **36** (2007), no. 2, 229–250.
[13] A. H. M. Murid and M. R .M. Razali, An integral equation method for conformal mapping of doubly connected regions, *Matematika* **15** (1999), no. 2, 79–93.
[14] A. H. M. Murid and L.-N. Hu, Numerical conformal mapping of bounded multiply connected regions by an integral equation method, *Int. J. Contemp. Math. Sci.* **4** (2009), no. 21–24, 1121–1147.
[15] M. M. S. Nasser, A boundary integral equation for conformal mapping of bounded multiply connected regions, *Comput. Methods Funct. Theory* **9** (2009), no. 1, 127–143.
[16] M. M. S. Nasser, Numerical conformal mapping via a boundary integral equation with the generalized Neumann kernel, *SIAM J. Sci. Comput.* **31** (2009), no. 3, 1695–1715.
[17] M. M. S. Nasser, Numerical conformal mapping of multiply connected regions onto the second, third and fourth categories of Koebe's canonical slit domains, *J. Math. Anal. Appl.* **382** (2011), no. 1, 47–56.
[18] M. M. S. Nasser, A. H. M. Murid, M. Ismail and E. M. A. Alejaily, Boundary integral equations with the generalized Neumann kernel for Laplace's equation in multiply connected regions, *Appl. Math. Comput.* **217** (2011), no. 9, 4710–4727.
[19] Z. Nehari, *Conformal Mapping*, McGraw-Hill, Inc., New York, Toronto, London, 1952.
[20] D. Okano, H. Ogata, K. Amano and M. Sugihara, Numerical conformal mappings of bounded multiply connected domains by the charge simulation method, *J. Comput. Appl. Math.* **159** (2003), no. 1, 109–117.
[21] L. Reichel, A fast method for solving certain integral equations of the first kind with application to conformal mapping, *J. Comput. Appl. Math.* **14** (1986), no. 1–2, 125–142.
[22] E. B. Saff and A. D. Snider, *Fundamentals of Complex Analysis*, Pearson Education, Inc. New Jersey, 2003.
[23] A. W. K. Sangawi, A. H. M. Murid and M. M. S. Nasser, Linear integral equations for conformal mapping of bounded multiply connected regions onto a disk with circular slits, *Appl. Math. Comput.* **218** (2011), no. 5, 2055–2068.
[24] G. T. Symm, Conformal mapping of doubly-connected domains, *Numer. Math.* **13** (1969), 448–457.
[25] R. Wegmann and M. M. S. Nasser, The Riemann-Hilbert problem and the generalized Neumann kernel on multiply connected regions, *J. Comput. Appl. Math.* **214** (2008), no. 1, 36–57.